

Research  
Glycomedicine—Article

## Fucosylated IgG Contributes to Adipose Tissue Dysfunction During Aging

Jingyu Wang<sup>a,#</sup>, Wei Su<sup>a,#</sup>, Haotian Wang<sup>b,#</sup>, Licui Liu<sup>a</sup>, Jinlong Li<sup>a,c,\*</sup>, Youxin Wang<sup>a,c,d,\*</sup><sup>a</sup> School of Public Health, North China University of Science and Technology, Tangshan 063210, China<sup>b</sup> School of Public Health, Capital Medical University, Beijing 100069, China<sup>c</sup> Hebei Key Laboratory of Organ Fibrosis, School of Public Health, North China University of Science and Technology, Tangshan 063210, China<sup>d</sup> Tangshan Key Laboratory of Clinical Epidemiology, School of Public Health, North China University of Science and Technology, Tangshan 063210, China

## ARTICLE INFO

## Article history:

Received 10 July 2025

Revised 30 September 2025

Accepted 13 October 2025

Available online 22 October 2025

## Keywords:

Immunoglobulin G

Fucosylation

Adipose tissue aging

Glycosylation

Metabolic dysfunction

Fibrosis

## ABSTRACT

Immunoglobulin G (IgG) is recognized as a key regulator of metabolic dysfunction and fibrosis in adipose tissue, and its functional properties are tightly regulated by its glycosylation profile. However, the role of IgG glycosylation in adipose aging remains unclear. Here, we performed transcriptomic and glycoproteomic analyses of epididymal white adipose tissue (eWAT) from young and aged mice. RNA sequencing (RNA-seq) analysis revealed a significant downregulation of adipogenic genes in aged eWAT, accompanied by elevated expression levels of inflammatory and fibrotic markers, which were further validated by quantitative polymerase chain reaction (qPCR). N- and O-glycoproteomic analyses revealed widespread changes in glycosylation. Differentially glycosylated proteins are primarily localized to the extracellular space and participate in innate immune responses, transport and signal transduction, extracellular matrix (ECM)–receptor interaction pathways, and so on. Notably, IgG glycosylation levels were significantly increased in aged mice. Specifically, the N-fucosylation of IgG1, IgG2a, and IgG3 was elevated by 3.1-, 10.4-, and 3.2-fold, respectively, while only IgG2a showed increased O-fucosylation. These findings suggest that N-fucosylation is a common age-related modification across IgG subtypes. Using *in vivo* models, we further demonstrated that B-cell depletion-induced IgG reduction increased adipogenic and inflammatory gene expression, while the expression of fibrotic markers was suppressed. These effects were reversed upon repletion with either fucosylated or nonfucosylated IgG. Importantly, compared with nonfucosylated IgG, fucosylated IgG exacerbated inflammation and fibrosis but inhibited adipogenesis more strongly. Taken together, our results identify fucosylated IgG as a key mediator of adipose dysfunction during aging and suggest that modulating IgG fucosylation may offer therapeutic potential for age-related metabolic disorders.

© 2025 THE AUTHORS. Published by Elsevier LTD on behalf of Chinese Academy of Engineering and Higher Education Press Limited Company. This is an open access article under the CC BY license (<http://creativecommons.org/licenses/by/4.0/>).

## 1. Introduction

Aging is a dynamic and complex biological phenomenon characterized by progressive functional decline across multiple organ systems [1]. The aging process and its associated chronic diseases have emerged as major contributors to human mortality [2]. Aging is commonly associated with widespread disruptions in metabolic homeostasis, which can lead to multiorgan dysfunction, threaten the health of the elderly population, reduce their quality of life, and impose a significant burden on health care systems. Therefore,

extending the healthspan and reducing the disease burden in older individuals remain major challenges in biomedical research.

Adipose tissue is a central metabolic and endocrine organ that is essential for maintaining systemic energy homeostasis, metabolic regulation, and immune balance [3,4]. Emerging evidence indicates that adipose tissue dysfunction is closely related to inflammation, fibrosis, and metabolic impairments during aging and is now recognized as a hallmark of the aging process [5–7]. Notably, white adipose tissue (WAT), the most prevalent adipose depot, is among the first tissues to undergo significant functional and structural changes with age [8,9]. Enhanced adipose tissue function is a common feature of several longevity-promoting interventions, such as caloric restriction [10], intermittent fasting [11], peroxisome proliferator-activated receptor  $\gamma$  (PPAR $\gamma$ ) activation [12], and elimination of senescent cells [13]. However, the underlying

\* Corresponding authors.

E-mail addresses: [lijinlong@ncst.edu.cn](mailto:lijinlong@ncst.edu.cn) (J. Li), [wangyouxin@ncst.edu.cn](mailto:wangyouxin@ncst.edu.cn) (Y. Wang).

# These authors contributed equally to this work.

mechanisms linking WAT dysfunction to aging remain incompletely understood.

Protein glycosylation, a critical posttranslational modification, directly influences immune homeostasis by modulating the function of proteins [14,15]. Immunoglobulin G (IgG) is a major serum glycoprotein and the predominant class of circulating antibodies. IgG glycosylation modulates its binding to Fc receptors (FcRs) and complement C1q, thereby regulating its biological activity. Altered IgG glycosylation patterns have been identified as promising biomarkers for aging and age-related diseases [16]. Moreover, IgG accumulates in WAT during aging, contributing to impaired adipose function and metabolic health [5]. However, whether glycosylation regulates the pro-aging effects of IgG in WAT remains to be elucidated.

In this study, we performed comprehensive N- and O-glycoproteomic profiling of adipose tissue to explore the effects of glycosylation on aging. We found that fucosylated IgG was significantly elevated in the epididymal WAT (eWAT) of aged mice. *In vivo* studies using complementary models revealed that fucosylated IgG plays a pivotal role in driving adipose tissue fibrosis and metabolic deterioration with aging, supporting its potential as a novel intervention target to improve metabolic health in older individuals.

## 2. Materials and methods

### 2.1. Animal experiments

The animal research was approved and guided by the Ethics Committee of North China University of Science and Technology, China (ethical number: 2024SY3060). All animal experiments were conducted in accordance with the *Animal Research: Reporting of In Vivo Experiments* guidelines.

Male C57BL/6J mice aged 2 and 18 months were obtained from the Model Organisms Center (China) and housed under specific pathogen-free (SPF) conditions.

The mice were divided into two age groups: young (2 months old,  $n = 5$ ) and aged (18 months old,  $n = 5$ ). eWAT was collected for RNA sequencing (RNA-seq), N-glycoproteomic, and O-glycoproteomic analyses.

For the *in vivo* IgG intervention study, 18-month-old male C57BL/6J mice ( $n = 5$  per group) were randomly divided into four groups: control, B-cell depletion, B-cell depletion + fucosylated IgG, and B-cell depletion + nonfucosylated IgG. The mice were intraperitoneally injected with 100  $\mu\text{g}$  of Rat IgG2b,  $\kappa$  Isotype Ctrl antibody (400644; BioLegend, USA) for control or anti-mouse CD20 antibody (SA271G2 clone; 152104; BioLegend) for B-cell depletion [17]. One week after B-cell depletion, the mice were intraperitoneally injected with 150  $\mu\text{g}$  of fucosylated or nonfucosylated human IgG1 (JOINN Biologics Co., Ltd., China) twice weekly for four weeks to replenish circulating IgG levels [18]. Since the production of glycosylated mouse IgG antibodies is currently not feasible, we applied human-derived IgG in the intervention because of its well-characterized glycoforms and its ability to bind to mouse Fc $\gamma$  receptors (Fc $\gamma$ Rs), enabling translational relevance and functional comparison with human immunometabolic studies. Fucosylated and nonfucosylated IgGs were expressed in wild-type Chinese hamster ovary (CHO) cells (CHO-K1) and fucosyltransferase *Fut8* knockout CHO cells (CHO<sup>*Fut8*-/-</sup>), respectively. Briefly, CHO<sup>*Fut8*-/-</sup> cells were established through clustered regularly interspaced short palindromic repeats (CRISPR)/CRISPR-associated protein 9 (Cas9)-mediated gene editing with life cycle assessment (LCA)-based selection. Following expansion, stable cell populations were grown in CD-CHO medium (Gibco, USA) in 1 L shaker flasks for a five-day period, after which the culture supernatants were

harvested. Human IgG1 was then isolated from the supernatant using affinity chromatography with a Protein A column (GE, USA). The eluted antibody was subsequently dialyzed into phosphate-buffered saline (PBS; pH 7.2) using a desalting column (GE) and concentrated using Amicon Ultra15 centrifugal devices (Millipore, USA). The purified monoclonal antibody was divided into aliquots and kept at  $-80\text{ }^{\circ}\text{C}$  until further use [19].

### 2.2. RNA-seq of eWAT

Total RNA was isolated from the eWAT of young ( $n = 3$ ) and aged ( $n = 5$ ) mice via TRIzol reagent (Invitrogen, USA). RNA quality was assessed via a NanoDrop 2000 spectrophotometer (Thermo Scientific, USA), and RNA integrity was further evaluated via an Agilent 2100 Bioanalyzer (Agilent Technologies, USA). Complementary DNA (cDNA) libraries were generated via the VAHTS Universal V6 RNA-seq Library Prep Kit (Vazyme, China), and sequencing was carried out on an Illumina NovaSeq 6000 platform (USA) in paired-end 150 bp mode.

The raw reads were filtered via fastp to eliminate low-quality sequences and adapter contaminants. High-quality reads were subsequently mapped to the mouse reference genome (GRCm39) with the aligner HISAT2. Transcript abundance was estimated via HTSeq-count, and principal component analysis (PCA) was performed in R (v.3.2.0) to assess sample grouping and reproducibility across biological replicates.

Differential gene expression analysis was conducted via DESeq2, with significance set at a false discovery rate (FDR)-adjusted  $P$ -value ( $P_{\text{adj}}$ )  $< 0.05$  and an absolute fold change (FC)  $> 2$ . The enrichment of biological functions and pathways among the differentially expressed genes (DEGs) was analyzed via Gene Ontology (GO) and Kyoto Encyclopedia of Genes and Genomes (KEGG) pathway annotations.

### 2.3. N- and O-glycoproteomic analysis of eWAT

For the N- and O-glycoproteomic analyses, eWAT samples (50 mg each) from both young ( $n = 5$ ) and aged ( $n = 5$ ) mice were individually processed. Each sample was homogenized in 500  $\mu\text{L}$  of ice-cold 8  $\text{mol}\cdot\text{L}^{-1}$  urea lysis buffer supplemented with 1 $\times$  ethylenediaminetetraacetic acid (EDTA)-free protease inhibitor cocktail (Report, China), followed by a 30 min incubation on ice to ensure complete protein extraction. After centrifugation at 14 100g for 20 min at 4  $^{\circ}\text{C}$ , the resulting supernatant was carefully collected. The protein concentration was subsequently quantified using the Bradford protein assay with bovine serum albumin as the standard.

The proteins were reduced with 10  $\text{mmol}\cdot\text{L}^{-1}$  tris(2-carboxyethyl) phosphine (TCEP) and alkylated with 25  $\text{mmol}\cdot\text{L}^{-1}$  chloroacetamide (CAA). Trypsin digestion was performed at a 50:1 protein-to-trypsin ratio overnight at 37  $^{\circ}\text{C}$ . The reaction was terminated with formic acid, and the peptides were desalted via a C18 column and lyophilized.

Glycopeptides were enriched via hydrophilic interaction liquid chromatography (HILIC). The HILIC column was equilibrated with 80% acetonitrile/1% trifluoroacetic acid (TFA), and the peptides were incubated with the packing material at 30  $^{\circ}\text{C}$  for 1 h. After centrifugation and washing, the glycopeptides were analyzed via a timsTOF-HT mass spectrometer in data-dependent acquisition (DDA) mode, with a mass range of 100–3500  $m/z$ .

The mobile phase consisted of phase A (0.1% formic acid in water) and phase B (80% acetonitrile and 0.1% formic acid). Gradient elution was performed as follows: 0–4 min, 5%–10% B; 4–46 min, 10%–24% B; 46–53 min, 24%–36% B; 53–54 min, 36%–95% B; and 54–60 min, 95% B.

Fragmented spectra were searched against the *Mus musculus* proteome database via Byonic software (v.2.13.17; Protein Metrics, USA). Separate glycan databases for N- and O-glycans were used for glycopeptide identification. A target–decoy approach was employed to control the FDR at 0.01. The raw data were median normalized to minimize experimental variability. Missing values were imputed via the Perseus algorithm after proteins with more than 50% missing values were filtered out. Differentially expressed glycosylation sites were identified on the basis of an average FC < 0.67 or > 1.5 and  $P < 0.05$ . Functional annotation and pathway analysis were conducted via the use of the GO and KEGG databases.

#### 2.4. Quantitative real-time reverse transcription polymerase chain reaction (qRT-PCR) analysis

Total RNA was reverse-transcribed into cDNA via an MF166-Plus kit (Mei5bio, China), and qRT-PCR was carried out with 2× SYBR quantitative polymerase chain reaction (qPCR) mix (Mei5bio). The relative expression levels of the target genes were calculated via the  $2^{-\Delta\Delta Ct}$  method, with normalization to the internal reference gene. The sequences of the primers used in this study are provided in Table S1 in Appendix A.

#### 2.5. Statistical analysis

We conducted a priori power analysis using G\*Power 3.1 software to determine sample sizes for *in vivo* experiments. On the basis of preliminary data showing an effect size of 1.2 (Cohen's  $d$ ) in metabolic parameters between age groups with type I error probability ( $\alpha$ ) = 0.05 and type II error probability ( $\beta$ ) = 0.20, the calculated minimum sample size was  $n = 5$  per group. This calculation accounted for the anticipated 20% attrition in aged mouse cohorts. Student's  $t$  test was used for comparisons between two experimental groups. One-way analysis of variance (ANOVA) followed by Tukey's post hoc test was used to compare three or more groups. The data were analyzed via GraphPad Prism 8, and  $P < 0.05$  was considered to indicate statistical significance.

### 3. Results

#### 3.1. Aged mice exhibit adipose tissue fibrosis, inflammation, and metabolic decline

Among various tissues, eWAT exhibits the most pronounced transcriptomic alterations during aging in mice [20]. Therefore, we performed RNA-seq profiling of eWAT to identify the transcriptomic alterations associated with aging (Fig. 1(a)). PCA score plots revealed clear separation between the two groups, indicating distinct transcriptomic profiles (Fig. 1(b)). A volcano plot revealed that compared with those of young mice, the eWAT of aged mice presented 1729 upregulated genes and 3128 downregulated genes (Fig. 1(c)).

GO analysis revealed that the DEGs were enriched in biological processes related to lipid metabolism, the inflammatory response, and immune system function (Fig. 1(d)). KEGG pathway analysis further revealed that the upregulated genes were enriched in inflammatory pathways (Fig. 1(e)), whereas the downregulated genes were predominantly associated with lipid metabolism pathways (Fig. 1(f)). Further analysis revealed that key adipogenic genes, including *Adipoq*, *Ppargc1a*, *Cfd*, and *Fasn*, were significantly downregulated in the eWAT of aged mice (Fig. 1(g)). In contrast, the expression levels of inflammatory markers such as *Ccl2*, *Tnf*, *Il1a*, and *Arg1* were significantly elevated (Fig. 1(g)).

Previous studies have shown that fibrosis of adipose tissue in aged mice is an important driving force for inflammation activation

and metabolic abnormalities [21]. Therefore, we also measured the expression of genes related to fibrosis. The RNA-seq data revealed that *Fn1*, *Pcolce2*, *Tgfb1*, and *Timp1* were significantly upregulated in the eWAT of aged mice (Fig. 1(g)). These findings were confirmed by qPCR analysis, which revealed consistent expression trends (Fig. 1(h)). Together, these results indicate that adipose tissue fibrosis, inflammation, and metabolic dysfunction are tightly linked to the aging process.

#### 3.2. N-glycoproteomic profile of eWAT from aged mice

Emerging evidence has revealed that IgG is an age-associated molecule capable of promoting adipose tissue fibrosis and metabolic dysfunction [5]. The functional properties of IgG are highly regulated by glycosylation. Furthermore, epidemiological studies have suggested that plasma IgG glycosylation patterns may serve as biomarkers of aging [16]. However, the glycosylation status of IgG in adipose tissue remains largely unexplored. To address this, we performed comprehensive N- and O-glycoproteomic profiling of eWAT from aged and young mice.

The N-glycoproteomic results are summarized in Fig. 2. PCA plots revealed clear separation between the two age groups (Fig. 2(a)), and volcano plots revealed significant differences in glycopeptide abundance (Fig. 2(b)). Compared with young mice, aged mice presented 640 upregulated and 570 downregulated glycopeptides. At the protein level, 148 proteins presented increased N-glycosylation, whereas 153 proteins presented decreased glycosylation in aged mice (Fig. 2(c)). Sequence motif analysis revealed NXS (N: asparagine, X: any amino acid except proline, S: serine; 42.56%) and NXT (T: threonine; 57.44%) as the predominant N-glycosylation sequons (Fig. 2(d)). Approximately 58.5% of the identified glycosylation sites (535 out of 914) were annotated in the UniProt database (Fig. 2(e)). Compared with young mice, aged mice presented elevated levels of sialylation and fucosylation, along with reduced oligomannose and complex/hybrid N-glycan types (Fig. 2(f)).

More than half of the identified glycoproteins (428 out of 598) contained only a single glycosylation site, whereas 64% of the glycosylation sites exhibited multiple glycans, indicating a high degree of glycan microheterogeneity (Fig. 2(g)). Glycans composed of 10–15 monosaccharide units were the most abundant in the dataset (Fig. 2(h)). A heatmap of glycan co-occurrences at the same glycosylation site revealed that sialylation frequently co-occurred with fucosylation and complex/hybrid glycans (Fig. 2(i)), suggesting site-specific glycan heterogeneity. GO and KEGG pathway analyses revealed that the differentially glycosylated proteins were primarily localized to the extracellular space (Fig. S1(a) in Appendix A), participated in innate immune responses (Fig. S1(b) in Appendix A), were involved in metal ion binding (Fig. S1(c) in Appendix A), and were enriched in the phagosome and extracellular matrix (ECM)–receptor interaction pathways (Fig. S1(d) in Appendix A), highlighting the functional relevance of glycosylation in age-related adipose dysfunction.

#### 3.3. O-glycoproteomic profile of eWAT from aged mice

The O-glycoproteomic results are presented in Fig. 3. PCA plots revealed clear separation between young and aged mice (Fig. 3(a)), and volcano plots revealed differential glycopeptide abundances (Fig. 3(b)). Compared with young mice, aged mice presented 85 upregulated and 163 downregulated glycopeptides. At the protein level, 39 proteins presented increased O-glycosylation, and 70 proteins presented decreased O-glycosylation in aged mice (Fig. 3(c)). Notably, none of the 687 quantified O-glycosylation sites were annotated in the UniProt database (Fig. 3(d)).

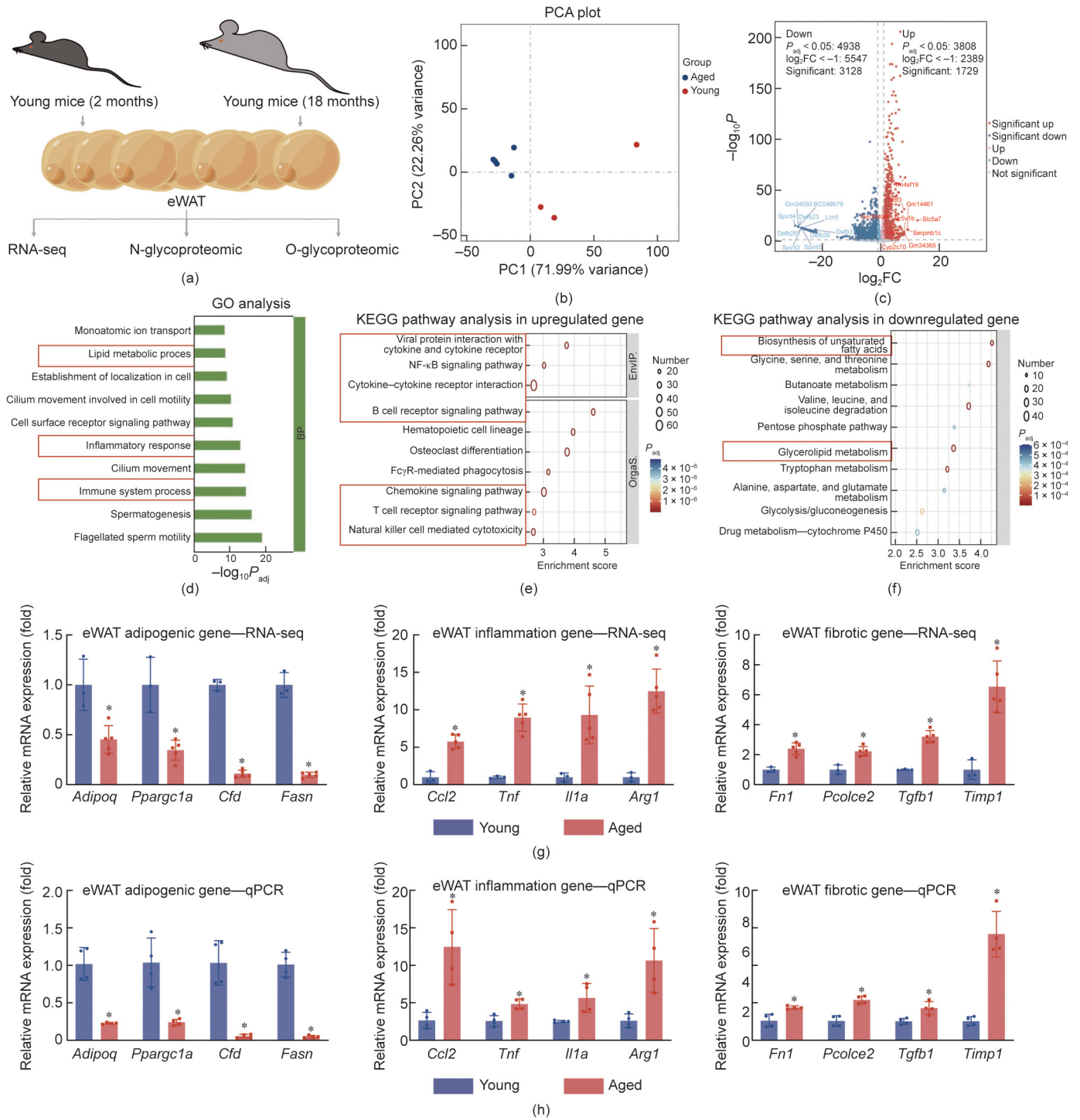


**Fig. 1.** Transcriptomic profiling of eWAT from young and aged mice. (a) Schematic diagram of the animal model. (b) PCA of eWAT samples from young ( $n = 3$ ) and aged ( $n = 5$ ) mice. (c) Volcano plot showing DEGs between the two groups ( $P < 0.05$ ,  $FC > 2$  or  $< 0.5$ ). (d) GO enrichment analysis of DEGs. (e, f) KEGG pathway analysis of (e) upregulated and (f) downregulated genes. (g) Expression levels of key adipogenic, inflammatory, and fibrotic genes in eWAT. (h) Validation of the expression of selected genes via qPCR ( $n = 4$  per group). The data are presented as the means  $\pm$  standard deviations (SDs). \* $P < 0.05$ , Student's  $t$  test. PC: principal component; EnvIP: environmental information processing; OrgaS: organismal systems; Metab: metabolism.

Sequence motif analysis revealed that O-glycosylation sites predominantly followed NXT (80.09%) or TT (19.91%) motifs, or, alternatively, NXS (57.41%), SN (24.78%), or NS (17.81%) motifs (Fig. 3(e)). Among the identified glycoproteins, 41% (100 out of 244) contained only a single glycosylation site, and 56.9% of all the sites presented multiple glycans, indicating significant glycan microheterogeneity (Fig. 3(f)). O-glycoproteomic data revealed that compared with young mice, aged mice presented increased

levels of sialylation, fucosylation, and high-mannose glycans but reduced levels of complex-type O-glycans (Fig. 3(g)). Glycans containing 8–12 monosaccharide units were most prevalent in the dataset (Fig. 3(h)).

However, owing to the structural complexity and irregularity of O-glycans, many could not be matched to entries in our O-glycan databases, limiting further classification. As a result, a glycan co-occurrence heatmap could not be generated. GO and KEGG

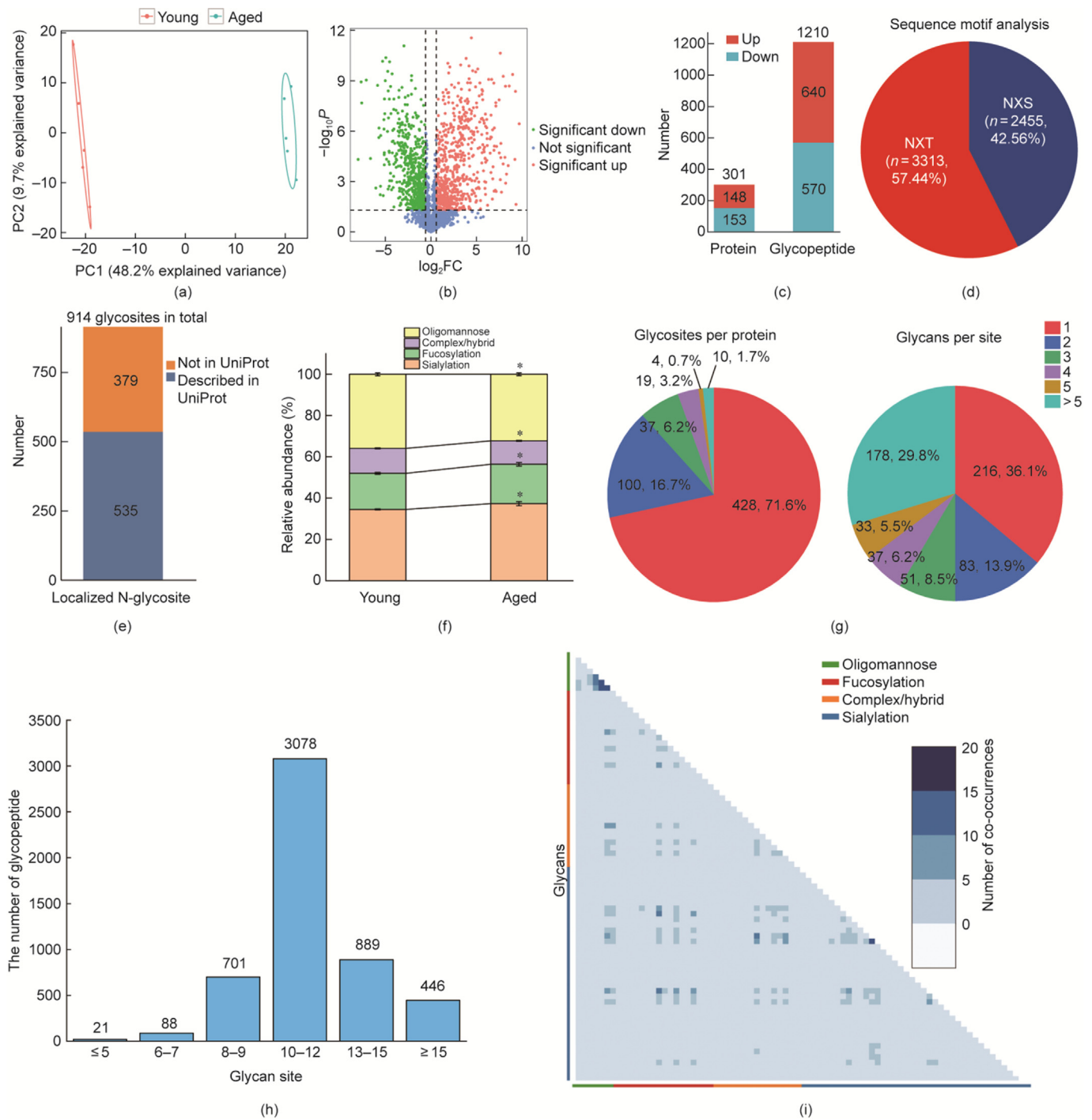


**Fig. 2.** N-glycoproteomic profiling of eWAT from young and aged mice. (a) PCA of N-glycoproteomic data from young ( $n = 5$ ) and aged ( $n = 5$ ) mice. (b) Volcano plot of differentially expressed glycopeptides ( $P < 0.05$ ,  $FC < 0.67$  or  $> 1.5$ ). (c) Numbers of differentially expressed proteins and glycopeptides identified via N-glycoproteomics. (d) Sequence motif analysis of N-glycosylation sites. (e) Annotation status of the quantified glycosylation sites in the UniProt database. (f) Distribution of N-glycan types between the two groups. The data are presented as the means  $\pm$  SDs ( $n = 5$  biological replicates; \* $P < 0.05$ ; Student's  $t$  test). (g) Distribution of N-glycosylation sites per protein and glycan microheterogeneity per site. (h) Glycan size distribution in eWAT-derived glycopeptides. (i) Glycan co-occurrence heatmap illustrating the frequency of glycan pairs at the same glycosylation site, indicating site-specific microheterogeneity.

analyses revealed that differentially glycosylated O-glycoproteins were enriched in the extracellular region (Fig. S2(a) in Appendix A), involved in transport and signal transduction (Fig. S2(b) in Appendix A), associated with metal ion binding (Fig. S2(c) in Appendix A), and linked to ECM receptor interaction pathways (Fig. S2(d) in Appendix A), suggesting a functional role for O-glycosylation in aging-related adipose tissue dysfunction.

### 3.4. Fucosylated IgG contributes to adipose tissue dysfunction and aging

We next examined whether IgG glycosylation levels were altered in aged mice. Our results revealed age-related changes in the glycosylation of the IgG1, IgG2a, and IgG3 subtypes (Table 1, Fig. S3 in Appendix A). Specifically, compared with that in young

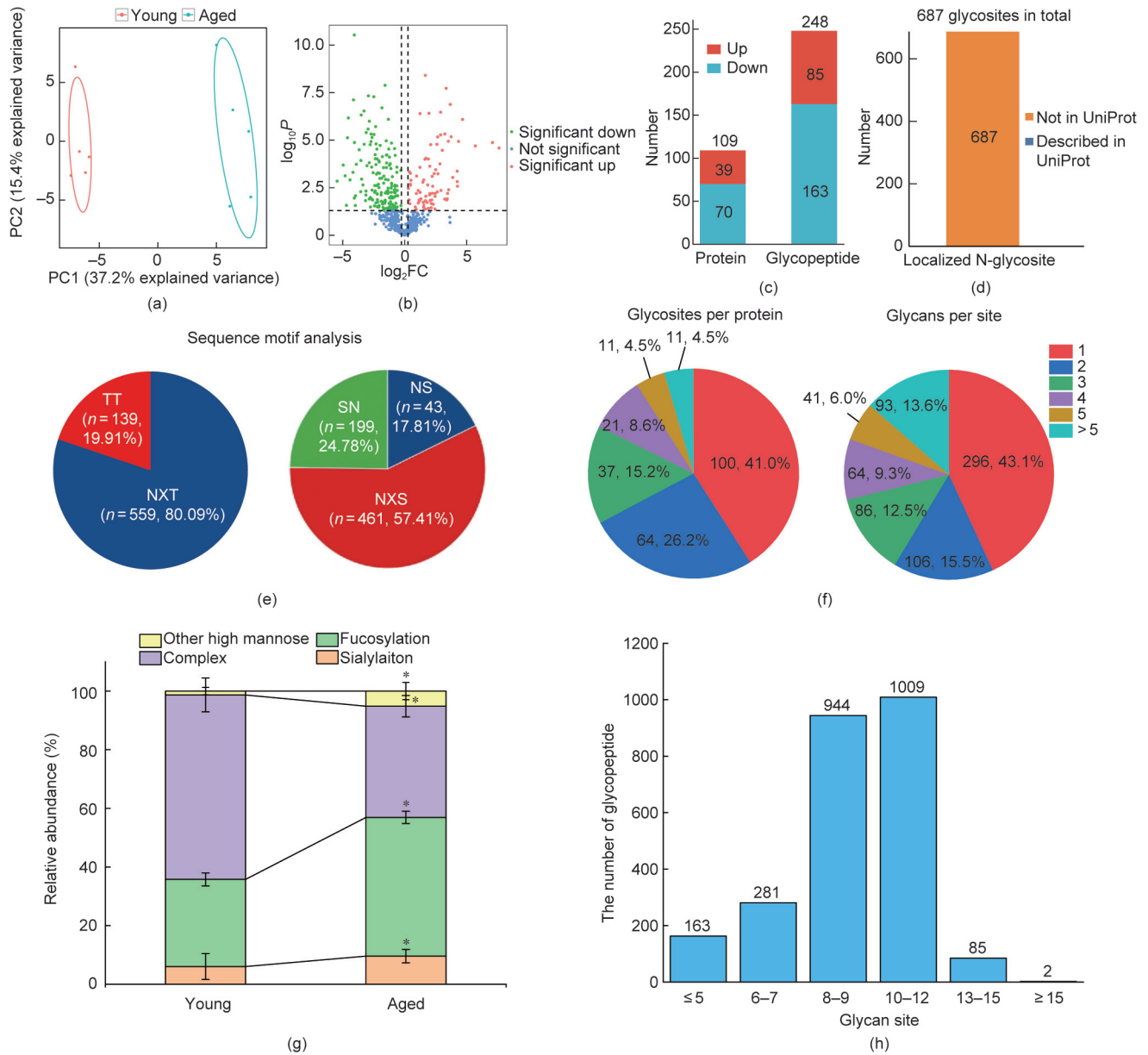


**Fig. 3.** O-glycoproteomic profiling of eWAT from young and aged mice. (a) PCA of O-glycoproteomic data from young ( $n = 5$ ) and aged ( $n = 5$ ) mice. (b) Volcano plot of differentially expressed glycopeptides ( $P < 0.05$ ,  $FC < 0.67$  or  $> 1.5$ ). (c) Numbers of differentially expressed proteins and glycopeptides identified via O-glycoproteomics. (d) Annotation status of quantified O-glycosylation sites in the UniProt database. (e) Sequence motif analysis of O-glycosylation sites. (f) Distribution of O-glycosylation sites per protein and glycan microheterogeneity per site. (g) Distribution of O-glycan types between the two groups. The data are presented as the means  $\pm$  SDs ( $n = 5$  biological replicates;  $*P < 0.05$ ; Student's  $t$  test). (h) Glycan size distribution in eWAT-derived O-glycopeptides.

controls, the N174 site of IgG1 in aged mice was modified with two fucosylations and one sialylation, with corresponding FCs of 3.097, 3.148, and 1.836, respectively. The N180 site of IgG2a was modified with three fucosylations, two sialylations, and one complex-type glycan. The most significantly altered glycan at this site was Hex(4)HexNAc(4)Fuc(1), whose expression changed 10.411-fold in aged mice compared to young mice. The N179 site of IgG3 was modified with three fucosylations, with FCs of 3.169, 3.052, and 1.847, indicating a pattern similar to that of IgG1. In terms of O-glycosylation, only IgG2a exhibited fucosylation at residues T182 and S181, with FCs of 9.453 and 10.789, respectively. These findings indicate that fucosylation is a commonly upregulated N-glycosylation feature across all three IgG subtypes during aging, suggesting a potential role for IgG fucosylation in age-related metabolic decline.

To investigate whether fucosylated IgG contributes causally to adipose tissue dysfunction, we employed an *in vivo* model (Fig. 4 (a)). As B cells are the primary source of IgG, we first depleted B cells and circulating IgG in aged mice with an anti-CD20 antibody. One week later, we administered either fucosylated or nonfucosylated human IgG1 to B-cell-depleted aged mice for four weeks to restore IgG levels.

Reduced adipogenic capacity is a characteristic feature of aging adipose tissue [22]. As expected, IgG elimination induced by B-cell depletion significantly upregulated the expression of adipogenic genes, including *Adipoq*, *Ppargc1a*, *Cfd*, and *Fasn*, in eWAT (Fig. 4 (b)). Consistently, the expression levels of inflammatory markers (*Ccl2*, *Tnf*, *Il1a*, and *Arg1*) and fibrotic genes (*Fn1*, *Pcolce2*, *Tgfb1*, and *Timp1*) were reduced (Figs. 4(c) and (d)). These effects caused by IgG depletion were reversed after four weeks of fucosylated and

**Table 1**  
Differential N- and O-glycans of the IgG subtypes.

Protein name	Glycan type	Glycan component	Position	FC	P value	Glycan group	Proposed structure
IgG1	N-glycans	Hex(4)HexNAc(4)Fuc(1)	N174	3.096682547	$2.56 \times 10^{-3}$	Fucosylation	
IgG1	N-glycans	Hex(5)HexNAc(4)Fuc(1)	N174	3.147924188	$2.82 \times 10^{-3}$	Fucosylation	
IgG1	N-glycans	Hex(5)HexNAc(4)NeuAc(1)	N174	1.836049682	$4.48 \times 10^{-3}$	Sialylation	
IgG2a	N-glycans	Hex(3)HexNAc(4)Fuc(1)	N180	7.273291822	$3.23 \times 10^{-5}$	Fucosylation	
IgG2a	N-glycans	Hex(4)HexNAc(4)Fuc(1)	N180	10.410833710	$1.94 \times 10^{-7}$	Fucosylation	
IgG2a	N-glycans	Hex(5)HexNAc(4)Fuc(1)	N180	6.034445183	$2.02 \times 10^{-3}$	Fucosylation	
IgG2a	N-glycans	Hex(5)HexNAc(4)NeuAc(1)	N180	6.047812172	$8.20 \times 10^{-4}$	Sialylation	
IgG2a	N-glycans	Hex(6)HexNAc(4)NeuAc(1)	N180	5.828319753	$1.42 \times 10^{-5}$	Sialylation	—
IgG2a	N-glycans	Hex(6)HexNAc(4)NeuAc(1)NeuGc(1)	N180	9.652621292	$1.54 \times 10^{-6}$	Complex	—
IgG3	N-glycans	Hex(3)HexNAc(4)Fuc(1)	N179	3.168719370	$9.20 \times 10^{-4}$	Fucosylation	
IgG3	N-glycans	Hex(4)HexNAc(4)Fuc(1)	N179	3.051891315	$2.11 \times 10^{-3}$	Fucosylation	
IgG3	N-glycans	Hex(5)HexNAc(4)Fuc(1)	N179	1.847491204	$7.12 \times 10^{-3}$	Fucosylation	
IgG2a	O-glycans	HexNAc(4)Hex(4)Fuc(1)	T182	9.453128698	$4.72 \times 10^{-6}$	Fucosylation	—
IgG2a	O-glycans	HexNAc(4)Hex(4)Fuc(1)	S181	10.789263810	$1.23 \times 10^{-2}$	Fucosylation	—

Green circle: mannose; yellow circle: galactose; blue square: HexNAc; purple diamond: sialic acid; red triangle: fucose.

nonfucosylated IgG treatment (Figs. 4(b)–(d)). Notably, compared with the B-cell depletion group (tagged as # if  $P < 0.05$ ; Figs. 4(b)–(d)) and the B-cell depletion + nonfucosylated IgG group (tagged as &sup8 if  $P < 0.05$ ; Figs. 4(b)–(d)), the B-cell depletion + fucosylated IgG group exhibited the most pronounced phenotypic effects. In particular, compared with nonfucosylated IgG, fucosylated IgG supplementation significantly suppressed adipogenesis while exacerbating inflammatory and fibrotic responses (Figs. 4(b)–(d)). These findings indicate that fucosylated IgG is a key driver of adipose tissue fibrosis and metabolic dysfunction during aging.

#### 4. Discussion

In this study, a transcriptomic analysis of eWAT from aged mice revealed that fibrosis, inflammation, and metabolic dysfunction of adipose tissue are closely associated with the aging process. WAT serves as a central metabolic and endocrine organ that plays a critical role in maintaining metabolic homeostasis during aging. Accumulating evidence has revealed that adipose tissue is a key driver of organismal aging and age-related pathologies [23]. Aging is associated with regional fat redistribution, the accumulation of senescent cells, fibrosis, and a diminished capacity for adipocyte differentiation, all of which impair adipose tissue function and contribute to systemic metabolic deterioration [24]. A recent prospective cohort study using full-length single-nucleus RNA sequencing (snRNA-seq) of human abdominal subcutaneous WAT revealed that older individuals exhibit dysregulated lipid metabolism, inflammatory phenotypes in insulin-responsive adipocytes, and increased immune responses linked to fibrosis across multiple cell populations, including preadipocytes, adipocytes, and vascular cells [25]. Compared with other major metabolic organs, adipose tissue shows earlier and more pronounced age-related transcriptomic changes, indicating its central role in aging-associated metabolic decline [20]. Moreover, immune cell infiltration in adipose tissue is a hallmark of aging [8], highlighting the complex interplay

between immune dynamics and adipose function. Significant fibrotic deposition is also observed in the adipose tissue of aging mice [5]. In our study, we also observed significant alterations in the expression of genes related to adipogenesis, inflammation, and fibrosis in eWAT from aged mice, which is consistent with these findings.

As one of the most abundant and structurally heterogeneous posttranslational modifications [26], glycosylation is involved in a wide range of biological and pathological mechanisms, including immune regulation, infectious diseases, neurodegeneration, and cancer [27]. Notably, changes in glycosylation patterns have been observed during aging. For example, altered fucosylation and sialylation in aged ovaries have been linked to immune activation [28], and widespread glycoproteomic changes in the aging heart, particularly in ECM-related and endoplasmic reticulum  $Ca^{2+}$ -binding proteins, have been associated with age-related cardiovascular dysfunction [29]. To investigate the functional relevance of glycosylation during aging, we conducted comprehensive N- and O-glycoproteomic profiling. The results revealed widespread changes in glycosylation in aged adipose tissue. Extracellular glycoproteins play essential roles in processes such as protein folding and stability, cell adhesion, and signaling [30]. Notably, in our study, the majority of glycosylation-modified proteins were also enriched in extracellular compartments and pathways related to inflammation (e.g., the innate immune response, proteolysis, integrin binding, and phagosome) and fibrosis (e.g., the ECM receptor interaction), further supporting a functional role for glycosylation in age-related adipose dysfunction.

Emerging evidence has highlighted IgG as a key mediator of adipose tissue metabolic reduction and degeneration during aging, and it is a potential therapeutic target for extending healthspan [5]. As one of the most extensively studied glycoproteins, the function of IgG is largely modulated by its glycosylation profile. Our previous observational studies have shown that IgG N-glycosylation is consistently associated with metabolic traits [31] and age-related diseases such as hypertension [32], hyperlipidemia

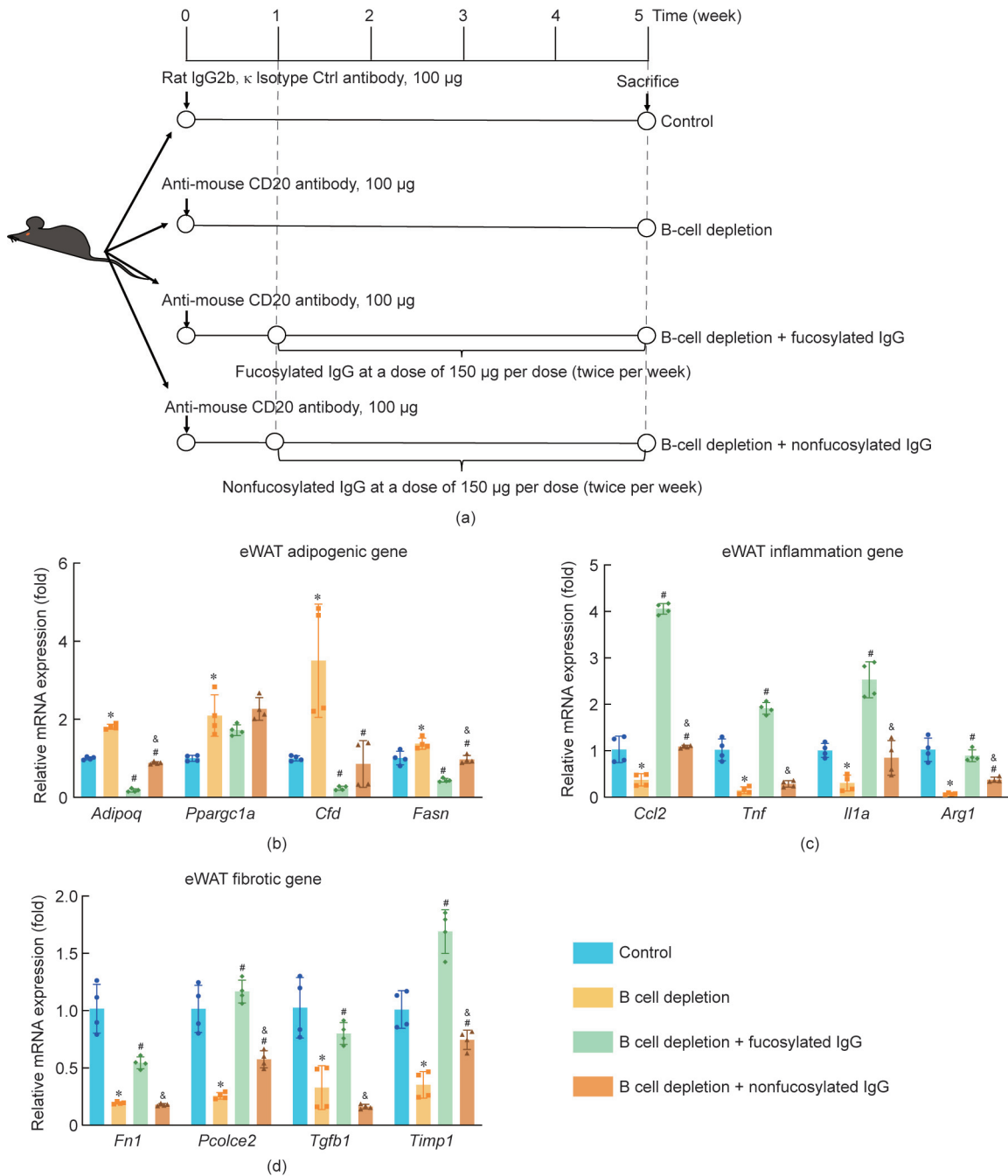


**Fig. 4.** Role of fucosylated IgG in eWAT dysfunction and aging. (a) Experimental design of the fucosylated and nonfucosylated IgG *in vivo* model in B-cell-depleted aged mice. (b–d) qRT-PCR analysis of the expression of key genes related to (b) adipogenesis, (c) inflammation, and (d) fibrosis in eWAT ( $n = 4$  for each group). The data are presented as the means  $\pm$  SDs. \* $P < 0.05$  vs the control group; # $P < 0.05$  vs the B-cell depletion group; & $P < 0.05$  vs the B-cell depletion + fucosylated IgG group (one-way ANOVA with Tukey's post hoc test).

[33], and type 2 diabetes [34]. An IgG N-glycosylation cardiovascular age has also been developed to track cardiovascular risk beyond calendar age [35]. In this study, we found that fucosylated IgG was significantly upregulated in the adipose tissue of aged mice. Multiple population studies have shown that IgG fucosylation is associated with aging, inflammation, obesity, and other diseases. Increased fucosylation of total IgG in serum was found to be associated with Down syndrome-induced premature aging [36] and autoimmune diseases such as systemic lupus erythematosus [37] and thyroid autoimmune disease [38]. Moreover, in obese patients, weight loss surgery induced a substantial decrease in core fucosylated IgG N-glycans in the serum, which is known to be associated

with a younger biological age and reflects an increased anti-inflammatory IgG potential [39]. Although our current study is based on a mouse model, these findings suggest that similar mechanisms occur in humans. We also propose that future studies should examine IgG glycosylation patterns in human adipose tissue or serum samples from aged or obese individuals.

IgG glycosylation can be modulated locally by the surrounding cellular microenvironment. A study based on an IgG N-glycosylation GWAS of 8090 individuals revealed that most tissues were enriched with specific IgG N-glycan traits [40]. Another study showed that adipose tissue from obese humans and mice contains T-bet<sup>+</sup> B cells that can locally secrete IgG to exacerbate metabolic

disorders during obesity [41]. Notably, core fucosylation was significantly increased during *in vivo* adipogenesis [42], suggesting the potential for local glycosylation. Moreover, weight loss in obese patients also induced a decrease in core fucosylated IgG N-glycans, which further indicates that fucosylated IgG may be derived from adipose tissue [39]. However, other tissues may also contribute to the production of fucosylated IgG during obesity or aging processes. For example, T-bet<sup>+</sup> B cells also accumulate in the spleens of obese mice [41]. In the livers of aging mice, the expression and activity of the fucosyltransferase Fut8 increase and are strongly linked to age-related changes in glycosylation [43]. In summary, regarding the local production or systemic derivation of fucosylated IgG, we acknowledge that this remains an open question and propose future experiments involving tissue-specific B-cell depletion or glycosylation profiling in multiple compartments to address this issue.

IgG fucosylation is associated with fibrosis development. Previous studies have shown that an increased degree of fucosylation of the IgG1 and IgG3 glycoforms is detected in patients with liver diseases [44], which are characterized by liver fibrosis. Core fucosylation leads to reduced binding to Fc $\gamma$ RIII and decreased antibody-dependent cellular cytotoxicity (ADCC) [45–47]. Natural killer (NK) cells are key mediators of the ADCC and target damaged cells, including aging cells [48]. The ADCC effect of NK cells may be impacted by fucosylated IgG, resulting in impaired clearance of aging cells. Excessive aggregation of aging cells can lead to fibrosis and tissue remodeling [49]. Therefore, the intervention of fucosylated IgG in this study promoted fibrosis, possibly because the fucose on the IgG Fc-glycan decreased Fc binding to Fc $\gamma$ RIII and thereby inhibited ADCC and the clearance of aging cells, ultimately promoting adipose tissue fibrosis. Among the mouse IgG subclasses, IgG2a/c is the most potent at mediating ADCC, followed by IgG2b and IgG1, whereas IgG3 has minimal ADCC activity because of its low affinity for Fc $\gamma$ Rs [50]. In our study, IgG2a exhibited the highest level of fucosylation, which may be linked to its dominant ADCC activity in mice. Our previous population studies also reported elevated IgG fucosylation in age-related conditions such as suboptimal health status [51] and central adiposity [52], reinforcing the role of fucosylated IgG in aging and age-associated pathologies.

Multiple advances have been made in therapeutic approaches targeting fucosylated IgG. For example, antibody glycoengineering by deletion of the *Fut8* gene could increase Fc $\gamma$ RIIIa binding affinity and lead to increased ADCC activity [53] and is widely applied in the clinic for the treatment of a wide range of diseases, especially cancer [54]. Moreover, the Fut8 inhibitor 2-fluorofucose (2FF) modulates the epidermal growth factor receptor (EGFR)–Janus kinase 1 (JAK1)–signal transducer and activator of transcription 3 (STAT3) signaling pathway by blocking core fucosylation, thereby enhancing antiviral interferon responses and suppressing RNA virus replication [55]. In summary, targeted fucosylated IgG has potential application value for aging and various diseases, such as immune diseases and cancer.

## 5. Limitations

This study has several limitations. First, the production of glycosylated mouse IgG antibodies is currently not feasible, limiting the use of endogenous IgG in our *in vivo* models. Notably, the human IgG1 subtype strongly binds to Fc $\gamma$ Rs and the complement system, a property comparable to that of murine IgG2a, making it a preferred isotype for both therapeutic applications and experimental studies [56]. Therefore, we utilized customized fucosylated and nonfucosylated human IgG1 antibodies in our complementary *in vivo* models. Second, the group size ( $n = 5$ ) was determined through rigorous power analysis and adheres to established guidelines in the field.

While this sample size is supported by previous studies and was sufficient to validate our key findings within the scope of this study [57,58], it may still limit our ability to detect subtler metabolic interactions or smaller effect sizes. Third, the upstream and downstream regulatory mechanisms of IgG fucosylation in aging adipose tissue remain unclear. Future *in vitro* studies are warranted to explore these molecular pathways in greater detail.

## 6. Conclusions

Our study revealed widespread alterations in both N- and O-glycosylation in aged adipose tissue. These changes are associated with metabolic dysfunction, chronic inflammation, and fibrosis in adipose tissue during aging. Notably, the N-fucosylation levels of IgG were markedly elevated in aged mice. Our *in vivo* experiments further suggest that the use of fucosylated IgG as a key mediator of adipose dysfunction during aging and nonfucosylated IgG may serve as a potential therapeutic strategy to mitigate age-related metabolic decline and extend healthspan.

## CRedit authorship contribution statement

**Jingyu Wang:** Writing – original draft, Visualization, Validation, Formal analysis. **Wei Su:** Writing – original draft, Visualization, Validation, Formal analysis. **Haotian Wang:** Writing – original draft, Visualization, Validation, Formal analysis. **Licui Liu:** Writing – review & editing, Investigation. **Jinlong Li:** Writing – review & editing, Project administration, Data curation. **Youxin Wang:** Writing – review & editing, Supervision, Funding acquisition, Conceptualization.

## Declaration of competing interest

The authors declare that they have no known competing financial interests or personal relationships that could have appeared to influence the work reported in this paper.

## Acknowledgments

This work was supported by the National Natural Science Foundation of China (82473717), the Natural Science Foundation of Hebei Province (H2024209024), and the Yanzhao Gold Talent Project of Hebei Province, China (HJZD202506).

## Appendix A. Supplementary data

Supplementary data to this article can be found online at <https://doi.org/10.1016/j.eng.2025.10.008>.

## References

- [1] Zhou Z, Yao J, Wu D, Huang X, Wang Y, Li X, et al. Type 2 cytokine signaling in macrophages protects from cellular senescence and organismal aging. *Immunity* 2024;57(3):513–527.e516.
- [2] Li R, Cheng X, Yang Y, Schwebel DC, Ning P, Li L, et al. Global deaths associated with population aging–1990–2019. *China CDC Wkly* 2023;5(51):1150–4.
- [3] Haberman ER, Sarker G, Arus BA, Ziegler KA, Meunier S, Martinez-Sanchez N, et al. Immunomodulatory leptin receptor(+) sympathetic perineurial barrier cells protect against obesity by facilitating brown adipose tissue thermogenesis. *Immunity* 2024;57(1):141–152.e5.
- [4] Li B, Li L, Li M, Lam SM, Wang G, Wu Y, et al. Microbiota depletion impairs thermogenesis of brown adipose tissue and browning of white adipose tissue. *Cell Rep* 2019;26(10):2720–2737.e5.
- [5] Yu L, Wan Q, Liu Q, Fan Y, Zhou Q, Skowronski AA, et al. IgG is an aging factor that drives adipose tissue fibrosis and metabolic decline. *Cell Metab* 2024;36(4):793–807.e5.
- [6] Yu Q, Xiao H, Jedrychowski MP, Schweppe DK, Navarrete-Perea J, Knott J, et al. Sample multiplexing for targeted pathway proteomics in aging mice. *Proc Natl Acad Sci USA* 2020;117(18):9723–32.

- [7] Zamboni M, Nori N, Brunelli A, Zoico E. How does adipose tissue contribute to inflammaging? *Exp Gerontol* 2021;143:111162.
- [8] Schaum N, Lehallier B, Hahn O, Palovics R, Hosseinzadeh S, Lee SE, et al. Ageing hallmarks exhibit organ-specific temporal signatures. *Nature* 2020;583(7817):596–602.
- [9] Sahu B, Bal NC. Adipokines from white adipose tissue in regulation of whole body energy homeostasis. *Biochimie* 2023;204:92–107.
- [10] Green CL, Lamming DW, Fontana L. Molecular mechanisms of dietary restriction promoting health and longevity. *Nat Rev Mol Cell Biol* 2022;23(1):56–73.
- [11] Liu S, Zeng M, Wan W, Huang M, Li X, Xie Z, et al. The health-promoting effects and the mechanism of intermittent fasting. *J Diabetes Res* 2023;4038546.
- [12] Xu L, Ma X, Verma N, Perie L, Pendse J, Shamloo S, et al. PPAR $\gamma$  agonists delay age-associated metabolic disease and extend longevity. *Aging Cell* 2020;19(11):e13267.
- [13] Wang L, Wang B, Gasek NS, Zhou Y, Cohn RL, Martin DE, et al. Targeting p21 (Cip1) highly expressing cells in adipose tissue alleviates insulin resistance in obesity. *Cell Metab* 2022;34(1):186.
- [14] Wang W. Glycomedicine: the current state of the art. *Engineering* 2023;26:12–5.
- [15] Wang W, Yang BF. The glycome and glycomedicine. *Engineering* 2023;26:1–2.
- [16] Wu Y, Zhang Z, Chen L, Sun S. Immunoglobulin G glycosylation and its alterations in aging-related diseases. *Acta Biochim Biophys Sin* 2024;56(8):1221–33.
- [17] Ercoli G, Ramos-Sevillano E, Nakajima R, de Assis RR, Jasinskas A, Goldblatt D, et al. The influence of b cell depletion therapy on naturally acquired immunity to streptococcus pneumoniae. *Front Immunol* 2020;11:611661.
- [18] Peng J, Vongpatanasin W, Sacharidou A, Kifer D, Yuhanna IS, Banerjee S, et al. Supplementation with the sialic acid precursor *N*-acetyl-*D*-mannosamine breaks the link between obesity and hypertension. *Circulation* 2019;140(24):2005–18.
- [19] Luo C, Chen S, Xu N, Wang C, Sai WB, Zhao W, et al. Glycoengineering of pertuzumab and its impact on the pharmacokinetic/pharmacodynamic properties. *Sci Rep* 2017;7(1):46347.
- [20] Zhou Q, Wan Q, Jiang Y, Liu J, Qiang L, Sun L. A landscape of murine long non-coding RNAs reveals the leading transcriptome alterations in adipose tissue during aging. *Cell Rep* 2020;31(8):107694.
- [21] Sun K, Tordjman J, Clément K, Scherer PE. Fibrosis and adipose tissue dysfunction. *Cell Metab* 2013;18(4):470–7.
- [22] Palmer AK, Kirkland JL. Aging and adipose tissue: potential interventions for diabetes and regenerative medicine. *Exp Gerontol* 2016;86:97–105.
- [23] Nguyen TT, Corvera S. Adipose tissue as a linchpin of organismal ageing. *Nat Metab* 2024;6(5):793–807.
- [24] Ahmed B, Farb MG, Gokce N. Cardiometabolic implications of adipose tissue aging. *Obes Rev* 2024;25(11):e13806.
- [25] Whytock KL, Divoux A, Sun Y, Pino MF, Yu G, Jin CA, et al. Aging human abdominal subcutaneous white adipose tissue at single cell resolution. *Aging Cell* 2024;23(11):e14287.
- [26] Schjoldager KT, Narimatsu Y, Joshi HJ, Clausen H. Global view of human protein glycosylation pathways and functions. *Nat Rev Mol Cell Biol* 2020;21(12):729–49.
- [27] Chatham JC, Patel RP. Protein glycosylation in cardiovascular health and disease. *Nat Rev Cardiol* 2024;21(8):525–44.
- [28] Wu Y, Zhang Z, Xu Y, Zhang Y, Chen L, Zhang Y, et al. A high-resolution N-glycoproteome landscape of aging mouse ovary. *Redox Biol* 2025;81:103584.
- [29] Franzka P, Kruger L, Schurig MK, Olecka M, Hoffmann S, Blanchard Y, et al. Altered glycosylation in the aging heart. *Front Mol Biosci* 2021;8:673044.
- [30] Steigmeyer AD, Lowery SC, Rangel-Angarita V, Malaker SA. Decoding extracellular protein glycosylation in human health and disease. *Annu Rev Anal Chem* 2025;18(1):241–64.
- [31] Meng XN, Cao WJ, Liu D, Elijah IM, Xing WJ, Hou HF, et al. Bidirectional causality between immunoglobulin G N-glycosylation and metabolic traits: a mendelian randomization study. *Engineering* 2023;26:2674–88.
- [32] Wang Y, Klarić L, Yu X, Thaqi K, Dong J, Novokmet M, et al. The association between glycosylation of immunoglobulin G and hypertension: a multiple ethnic cross-sectional study. *Medicine* 2016;95(17):e3379.
- [33] Liu D, Chu X, Wang H, Dong J, Ge SQ, Zhao ZY, et al. The changes of immunoglobulin G N-glycosylation in blood lipids and dyslipidaemia. *J Transl Med* 2018;16(1):235.
- [34] Meng X, Wang F, Gao X, Wang B, Xu X, Wang Y, et al. Association of IgG N-glycomics with prevalent and incident type 2 diabetes mellitus from the paradigm of predictive, preventive, and personalized medicine standpoint. *EPMA J* 2023;14(1):1–20.
- [35] Wu ZY, Guo Z, Zheng YL, Wang YT, Zhang HP, Pan HY, et al. IgG N-glycosylation cardiovascular age tracks cardiovascular risk beyond calendar age. *Engineering* 2023;26:99–107.
- [36] Streng BMM, Van Coillie J, Wildenbeest JG, Binnendijk RS, Smits G, den Hartog G, et al. IgG1 glycosylation highlights premature aging in Down syndrome. *Aging Cell* 2024;23(7):e14167.
- [37] Sjowall C, Zapf J, von Lohneysen S, Magorivska I, Biermann M, Janko C, et al. Altered glycosylation of complexed native IgG molecules is associated with disease activity of systemic lupus erythematosus. *Lupus* 2015;24(6):569–81.
- [38] Trzos S, Link-Lenczowski P, Sokolowski G, Pochec E. Changes of IgG N-glycosylation in thyroid autoimmunity: the modulatory effect of methimazole in graves' disease and the association with the severity of inflammation in Hashimoto's thyroiditis. *Front Immunol* 2022;13:841710.
- [39] Greto VL, Cvetko A, Stambuk T, Dempster NJ, Kifer D, Deris H, et al. Extensive weight loss reduces glycan age by altering IgG N-glycosylation. *Int J Obes* 2021;45(7):1521–31.
- [40] Li X, Wang H, Zhu Y, Cao W, Song M, Wang Y, et al. Heritability enrichment of immunoglobulin G N-glycosylation in specific tissues. *Front Immunol* 2021;12:741705.
- [41] Hagglof T, Vanz C, Kumagai A, Dudley E, Ortega V, Siller M, et al. T-bet<sup>+</sup> B cells accumulate in adipose tissue and exacerbate metabolic disorder during obesity. *Cell Metab* 2022;34(8):1121–1136.e6.
- [42] Wongtrakul-Kish K, Herbert BR, Packer NH. Bisecting GLCNAC protein N-glycosylation is characteristic of human adipogenesis. *J Proteome Res* 2021;20(2):1313–27.
- [43] Vanhooren V, Dewaele S, Kuro OM, Taniguchi N, Dolle L, van Grunsven LA, et al. Alteration in N-glycomics during mouse aging: a role for Fut8. *Aging Cell* 2011;10(6):1056–66.
- [44] Yuan W, Sanda M, Wu J, Koomen J, Goldman R. Quantitative analysis of immunoglobulin subclasses and subclass specific glycosylation by LC-MS-MRM in liver disease. *J Proteomics* 2015;116:11624–33.
- [45] Chen CL, Hsu JC, Lin CW, Wang CH, Tsai MH, Wu CY, et al. Crystal structure of a homogeneous IgG-Fc glycoform with the N-glycan designed to maximize the antibody dependent cellular cytotoxicity. *ACS Chem Biol* 2017;12(5):1335–45.
- [46] Biermann MH, Griffante G, Podolska MJ, Boeltz S, Sturmer J, Munoz LE, et al. Sweet but dangerous—the role of immunoglobulin G glycosylation in autoimmunity and inflammation. *Lupus* 2016;25(8):934–42.
- [47] Le NP, Bowden TA, Struwe WB, Crispin M. Immune recruitment or suppression by glycan engineering of endogenous and therapeutic antibodies. *Biochim Biophys Acta Gen Subj* 2016;1860(8):1655–68.
- [48] Shin E, Bak SH, Park T, Kim JW, Yoon SR, Jung H, et al. Understanding NK cell biology for harnessing NK cell therapies: targeting cancer and beyond. *Front Immunol* 2023;14:1192907.
- [49] Schafer MJ, White TA, Iijima K, Haak AJ, Ligresti G, Atkinson EJ, et al. Cellular senescence mediates fibrotic pulmonary disease. *Nat Commun* 2017;8(1):14532.
- [50] Wohnner M, Nimmerjahn F. Cytotoxic IgG: mechanisms, functions, and applications. *Immunity* 2025;58(6):1378–95.
- [51] Meng X, Wang B, Xu X, Song M, Hou H, Wang W, et al. Glycomic biomarkers are instrumental for suboptimal health status management in the context of predictive, preventive, and personalized medicine. *EPMA J* 2022;13(2):195–207.
- [52] Liu D, Li Q, Dong J, Li D, Xu X, Xing W, et al. The association between normal BMI with central adiposity and proinflammatory potential immunoglobulin G N-glycosylation. *Diabetes Metab Syndr* 2019;12:2373–85.
- [53] Grav LM, Lee JS, Gerling S, Kallehauge TB, Hansen AH, Kol S, et al. One-step generation of triple knockout CHO cell lines using CRISPR/Cas9 and fluorescent enrichment. *Biotechnol J* 2015;10(9):1446–56.
- [54] Butler M, Meneses-Acosta A. Recent advances in technology supporting biopharmaceutical production from mammalian cells. *Appl Microbiol Biotechnol* 2012;96(4):885–94.
- [55] Pan Q, Xie Y, Zhang Y, Guo X, Wang J, Liu M, et al. EGFR core fucosylation, induced by hepatitis C virus, promotes TRIM40-mediated-RIG-I ubiquitination and suppresses interferon-I antiviral defenses. *Nat Commun* 2024;15(1):652.
- [56] Nimmerjahn F, Vidarsson G, Cragg MS. Effect of posttranslational modifications and subclass on IgG activity: from immunity to immunotherapy. *Nat Immunol* 2023;24(8):1244–55.
- [57] Bhargava R, Upadhyay R, Zhao C, Katakam P, Wenderfer S, Chen J, et al. Aberrant glycosylation of IgG in children with active lupus nephritis alters podocyte metabolism and causes podocyte injury. *Arthritis Rheumatol* 2025;77(10):1421–32.
- [58] Alfaras I, Ejima K, Vieira Ligo Teixeira C, Di Germanio C, Mitchell SJ, Hamilton S, et al. Empirical versus theoretical power and type I error (false-positive) rates estimated from real murine aging research data. *Cell Rep* 2021;36(7):109560.